PHOTOGRAPH THIS SHEET

AD A951390

DTIC ACCESSION NUMBER

LEVEL

INVENTORY

Cornell Aeronautical Lab, Inc
Buffalo, NY

Rept. No. CAL-UB-1088-P-100

DOCUMENT IDENTIFICATION

Contract DA30-115-ORD-739

9 Jan. 57

DISTRIBUTION STATEMENT A
Approved for public release;
Distribution Unlimited

DISTRIBUTION STATEMENT

ACCESSION FOR		
NTIS	GRA&I	☒
DTIC	TAB	☐
UNANNOUNCED		☐
JUSTIFICATION		
(9 Jan. 1957)		
BY Per DTIC Form 50		
DISTRIBUTION / on file		
AVAILABILITY CODES		
DIST	AVAIL AND/OR SPECIAL	
A		

DISTRIBUTION STAMP

Released

DTIC
ELECTE
OCT 1 1981
S D
D

DATE ACCESSIONED

Acq. #81-2389
10 Sep. 81

UNANNOUNCED

DATE RECEIVED IN DTIC

PHOTOGRAPH THIS SHEET AND RETURN TO DTIC-DDA-2

DTIC FORM OCT 79 70A

DOCUMENT PROCESSING SHEET

CORNELL AERONAUTICAL LABORATORY, INC.

Project RUBY
Report No. UB-1088-P-100

Errors in the Measurement of Radar Echoing Patterns: A New Minimum Range Criterion

by

W. P. Malling

Contract DA-30-115-ORD-739

9 January 1957

4

B U F F A L O ,

FORM 144-A

CORNELL AERONAUTICAL LABORATORY, INC.

BUFFALO, N. Y.

REPORT NO. UB-1088-P-100

Errors in the Measurement of Radar
Echoing Patterns: A New Minimum
Range Criterion

by

W. P. Melling

Project RUBY
Contract DA-30-115-ORD-739

Prepared by:

W. P. Melling

W. P. Melling
Associate Electronics Engineer

Approved by:

Robert E. Kell

Robert E. Kell
Principal Physicist

Seville Chapman

Seville Chapman, Head
Physics Department

9 January 1957

FORM 145-A

CORNELL AERONAUTICAL LABORATORY, INC.

BUFFALO, N. Y.

PREPARED BY W. P. Melling REPORT NO. UB-1088-P-100

Project RUBY is a program of theoretical and experimental investigations of missile radar cross sections. Because of the importance of this topic, we plan to issue a series of occasional reports and working papers presenting our ideas and knowledge on various phases of the problem at the date of issue. It is hoped these papers will stimulate constructive comments and criticisms by workers in the field.

FORM 145-A

CORNELL AERONAUTICAL LABORATORY, INC.

BUFFALO, N. Y.

PREPARED BY W. P. Melling REPORT NO. UB-1068-P-100

Abstract

A formulation is provided of the target range required for satisfactory measurement of echoing area in a radar test site. When a conventional antenna is used against a target larger than about 10 wavelengths the necessary range is usually given by pD_p^2/λ, where D_p is the maximum projected target model dimension seen by the antenna, λ the test wavelength, and p a constant (of the order of 3) which effectively defines the quality of measurement. This formulation may fail when the target is near the end-on position, when the test range should not be made less than 5p times the length of the target. The validity of the criterion is not yet established for cases where it indicates that the target be placed in the near zone of the antenna.

TABLE OF CONTENTS

LIST OF FIGURES

FORM 145-A

CORNELL AERONAUTICAL LABORATORY, INC.

BUFFALO, N. Y.

PREPARED BY W. P. Melling REPORT NO. UB-1088-P-100

Introduction

Knowledge of the echoing area of the target is essential to the radar designer, and the most direct method of obtaining it is by measurement of the radar return from the target itself, or from a model. If the model can be supported in any required aspect and a radar is available, the only reassurance needed is that the measured echoing area will then be substantially the same as that which would be observed if the target were at the very long range associated with normal detection. That this may not be the case is evident, for at long range the illuminating wavefront is practically flat whereas at short range it is spherical or worse. The distance between test radar and target model must be made large enough for this effect, and other phenomena associated with the proximity of the antenna, to be small. "Far zone criteria" have been proposed in the past to specify a sufficient test range (e.g., Reference 1). These generally have the form:

$$\text{Range} \geq \text{constant} \times \frac{(D + d)^2}{\lambda}$$

where D is the model span, d the antenna diameter and λ the test wavelength. Their justification is that they specify a range such that the phase shift in the longest propagation path between antenna and model does not differ from that in the shortest path by more than a certain fraction of a wavelength (specified by the constant). The objection to such formulae is that because they consider only two extreme propagation paths rather than radiation from the whole antenna, they are wrong and, while this in itself may be of little moment (for any formula is better than none at all), the fact that they lead to requirements for huge test ranges against large targets is serious. For example, even if the constant in the formula is only unity and a very small antenna is used, a range of a mile is required using an X-band radar against a 230 wavelength target, and this figure would be quadrupled if the antenna diameter were made equal to the model span. In addition to a high cost for real estate, a long range implies costly supporting structures since the beam must be elevated to minimize ground reflection. For example, a 500 foot target elevation would be required, with even higher supporting towers, if a 5 degree beam were used against a target a mile away. Furthermore, the longer the range the less the system sensitivity. Such are the considerations which have prompted a reassessment of test range requirements and this report considers primarily the factors determining that range when the model is fairly large -- greater than 10 wavelengths.

It will be assumed that a conventional radar antenna is to be employed. While it may be possible to design a special antenna capable of reproducing at close range the plane wave fronts and uniform illumination associated with a distant region, such a development could not be justified unless it could be shown to have advantages over a conventional system. In particular the requirement for uniform field is unlikely to be compatible with a low level of side lobes. Since it is possible that measurement sensitivity may be limited by ground clutter,[2] this may be an overriding consideration. The present report provides a measure against which the advantages of range reduction by such an antenna may be assessed.

As the test range is increased the measured echoing pattern will approach asymptotically the range-independent form associated with the free space target. Thus before the minimum test range can be defined a judgment must be made of how great a deviation from the free space pattern is tolerable. Such a judgment must depend on circumstances -- in some cases it might be desirable to employ a shorter range than pattern distortion considerations alone would suggest, so as to buy sensitivity or economize on real estate. The line of attack followed in this report is to postulate a simplified form of target, compute the form of pattern that would be measured at a number of ranges by a radar whose antenna size is variable, and to use these results to establish more general formulae for test range as a function of model size, aspect, and test wavelength. With some reservations, to be expanded in a later report, it will be shown that antenna diameter has little influence on the measurement, provided it is less than the model span. It will be shown that if the echoing pattern of a target in the broadside aspect is determined at a given range, it is possible to derive expressions for the range necessary to maintain the same pattern quality when the target is in any other aspect, provided the test antenna is smaller than the model. For targets larger than about ten wavelengths it is possible to demonstrate that the quality of the detailed pattern associated with a range pD_p^2/λ, where D_p is the maximum projected dimension of the target and p a constant, is independent of aspect except when the target is nearly end-on. The number p is in fact a measure of the quality of pattern measurement, and an acceptable value may be determined by examining a set of broadside patterns taken or computed at various ranges. If the model then has a maximum span D, and the minimum range R for satisfactory measurement may be expressed as $R = p_1 D^2/\lambda$, the employment of p_1 in the pD_p^2/λ formula will indicate an adequate range for any other target aspect. It will be shown that this rule fails near the end-on aspect only if it requires a range of less than $5pD$.

In the establishment of this range rule it has been assumed that a target may be represented by an array of point scatterers. This simplification sidesteps the very difficult problem of analyzing the electromagnetic field associated with a continuous target. Two justifications of the procedure are possible:

1. In many targets the prime sources of scattered energy are relatively localized.

2. There is no such thing as a typical target, and it is reasonable to consider a worst case in the present analysis. From this point of view a case where a large proportion of scattered energy emanates from points at the target extremes provides an excellent model.

Accordingly, the returns from targets containing both five and three scatterers are examined.

The RF Field near an Antenna

The field of an antenna may be broadly separated into three regions:

(a) The far zone, where all wave fronts are spheres centered on the antenna, and where over a limited distant region such as that occupied by a target, signal amplitude may be assumed constant and the wavefront planar.

(b) The inductive field extending from the antenna to a range of a few wavelengths. This is insufficiently representative of the target region to be used for echoing area measurement.

(c) An intermediate region, vaguely called the near zone, in which the energy is purely electromagnetic radiation, but where the assumption of a plane uniform wave front cannot be made. It extends from the limit of the inductive field to a range of a few times d^2/λ, where d is the antenna diameter and λ the wavelength. For example, its extent would be a few hundred feet with a 3 foot diameter X-band antenna.

The present requirement is for as short a range as possible, and the question of how close into the intermediate region it is possible to operate must be answered. The first stage of analysis will be therefore to define the field at intervals through this region. The task is simplified by the fact that at ranges greater than a few wavelengths a scalar representation of the field is adequate,[3] and because of the necessary crudity of the target models considered in the next section it was not felt worth while to postulate a more complicated antenna than a linear uniformly illuminated one-dimensional aperture.

The geometry used in the field derivation is shown in Figure 1. To determine the deviation from uniformity of the field along a normal to the antenna axis, it is simply necessary to formulate for each point on this normal the complex sum of amplitude contributions from every point on the antenna. The radiation exciting a scatterer located at such a point on the normal may then be represented as a vector having a defined amplitude attenuation and phase angle with respect to signal transmitted by the antenna. If the signal received by the antenna as a result of re-radiation is to be computed, the return signal will be further reduced by the same attenuation coefficient and subjected to the same phase delay as in the outgoing path. Thus, if a scatterer is assumed to re-radiate all the energy incident upon it with zero phase shift, the received signal may be represented by a vector with a phase angle of twice the one-way phase shift, and having an amplitude defined by the square of the one-way attenuation term.

Analysis of the form of the field has been normalized against the maximum target model dimension D. This dimension is employed since, once the test wavelength is fixed, it is determined absolutely by a requirement to measure the echoing area of a given target as seen by a given radar. The antenna diameter d, which might have been used as the normal dimension, may be varied by the system designer, and will be defined by a variable c, such that:

$$d = cD$$

Then the distance from the axis of the point at which the field is to be determined may be defined by a normalized parameter α , where

$$\alpha = 2 \times \frac{\text{distance of point of measurement from antenna axis}}{\text{Model span } D}$$

As may be seen from Figure 1, dimensionless expressions for the field are then obtained if the range at which the field is to be defined is described by a parameter p, such that

$$\text{Range} = \frac{pD^2}{\lambda}$$

where λ is the test wavelength.

The field across a normal distance equal to the model span has been computed for a number of ranges in the vicinity of D^2/λ . The associated values of p (whose particular numerical values were chosen on the basis of manipulative convenience) lie between 0.125 and 5.56. So that the effect of changing the antenna size may be visualized, the field at each value of p was computed for an antenna diameter cD of zero, 0.6D and 1.0D. There is no significance in the choice of 0.6 rather than any other fraction as the intermediate value of c. The results are given in Figures 2-5 in terms of the signal that would be received from a unit scatterer at a point displaced from the axis by $\alpha D/2$.

First consider Figure 2, in which is plotted the received phase and amplitude for a scatterer at a range $D^2/8\lambda$ (p = 0.125). For equal antenna and model spans (c = 1) the phase of the return has a fine structure, although its absolute excursion from zero is not large. The variation in amplitude return as the scatterer is moved across the axis is considerable (more than 15 db), especially toward the edge of the field. With a smaller antenna (c = 0.6) both the phase and amplitude variations are increased, the former approaching the spherical wave front (dotted curve) associated with a point radiator. When p is increased to 0.5 (Figure 3) a relatively flat wave front having less fine structure than in the previous case is maintained with the largest antenna (c = 1.0). But as the scatterer is moved normal to the axis a variation of 20 db in its return must be expected. Reduction of the antenna diameter to 0.6D results in a decrease in amplitude error, but at the same time the phase deviation increases to become nearly as great as that from a point antenna.

At a range D^2/λ (p = 1.0; see Figure 4) both phase and amplitude vary monotonically. The amplitude variation is less than for smaller ranges, but is still considerable. When the antenna diameter and model span are equal, the phase deviation nearly coincides with that from the point source, and with the smaller antenna coincidence is practically complete. In fact, provided the antenna is no larger than the model, it is a sufficient approximation to assume the wave front spherical at all ranges greater than D^2/λ. Then the received phase lag ϕ from an off-axis scatterer may be readily shown (Appendix A) to be given in terms of normalized lateral displacement α and normalized range p by

$$\phi = 90^\circ \frac{\alpha^2}{p} \tag{1}$$

The dependence of amplitude upon p and α cannot be so simply expressed, and it is plotted for values of p from 2 to 5.56 in Figure 5. Because with increasing range a model of span D occupies a decreasing proportion of the antenna beamwidth (approximately D/R : λ/d = c/p times the nominal beamwidth), the amplitude variation becomes very small when the antenna diameter is no larger than the model span and the test range is greater than $3D^2/\lambda$.

The Measured Echoing Pattern of a Simplified Target

The re-radiation from a target arises from the currents set up in its skin by an incident field, and insofar as in many cases the effects of such currents predominate in isolated areas, a target may be regarded to a first approximation as an array of independent point scatterers. If this assumption is granted, the results of the preceding section allow a derivation of the echoing pattern which would be measured against a fully specified target at a finite range. The procedure will now be followed of developing a series of echoing patterns of such a target, so that the effect of changing the measurement range may be observed. It is assumed that effects resulting from modification of the antenna illumination by the target are negligible at ranges suitable for measurements against the relatively large targets considered here.

In order to keep the computations within bounds (and because there is no "typical" target in these terms) a very simple target structure has been chosen. It consists of only five points, each of which is assumed to re-radiate the same fraction of the incident radiation, with zero phase shift. Its arrangement is shown below.

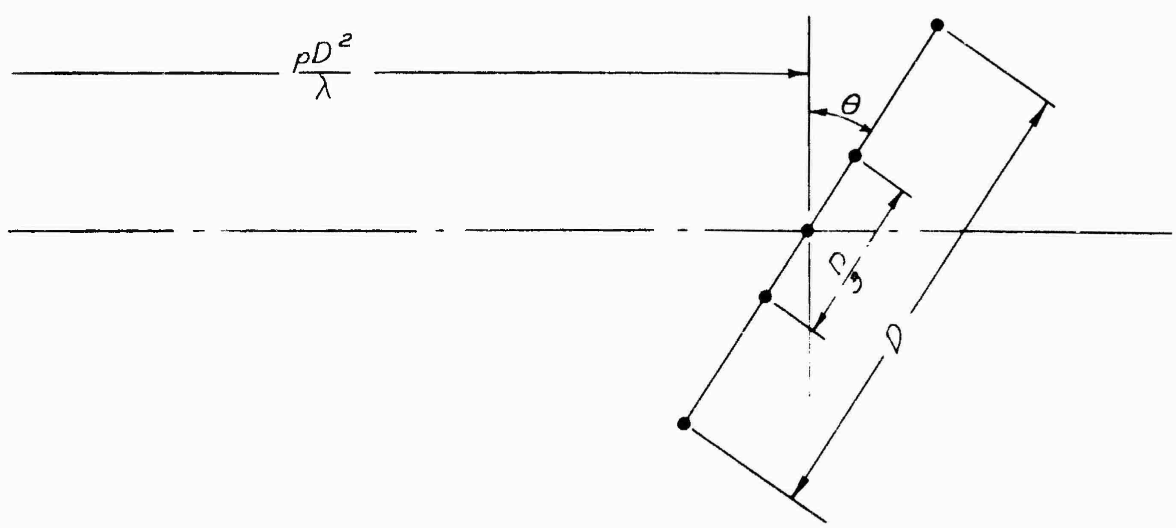

First the pattern obtained with the target near the broadside position will be considered. Target rotation results in differential changes in path lengths between the antenna and the separate scatterers producing an interference pattern (Figures 6 and 7) which would in this case exhibit absolute nulls if the target were viewed from an infinite distance (see Figure 6a). The curvature of the incident phase fronts at closer approach introduces a phase error in the returns from the outer scatterers, which prevents the absolute signal cancellation observed at an infinite range. In the computation of the patterns for such closer ranges it has been assumed that the model is sufficiently large for more than a cycle of the pattern to be developed with a very small angular rotation. This simplification implies:

(a) That there is no significant movement of the outer scatterers toward the antenna axis with the small model rotation considered, so that the relative intensity of returns from these scatterers is not modified by any excursion through details of the field structure. With this proviso it is possible to normalize rotation independently of model size to an angle equal to the physical rotation times D/λ.

(b) That rotation causes insufficient movement of the scatterers in range for it to be necessary to account for changes in the received signal resulting from over-emphasis of returns from the nearer scatterers (the radar fourth power law effect).

It is seen from Figure 6 that even at a range of $10D^2/\lambda$, a free space null appears as a finite signal 27 db below the highest maximum in the pattern, while at $3D^2/\lambda$ the ratio of minimum to maximum is only 17 db. Comparison of the left hand and right hand halves of Figure 6d, which show respectively the patterns using point and full size ($c = 1$) antennae, indicates for the latter that as close as $3D^2/\lambda$ the fall-off in return amplitude from target extremes has little effect on the pattern. However, such an effect is very apparent when p is less than 2.

At a range of D^2/λ ($p = 1$) the quality of the pattern is poor, especially for the larger antenna, where the reduced amplitude of returns from the target extremes results in suppression of the structure associated with the outer scatterers. At shorter ranges the patterns lose all resemblance to that from free space.

A further set of patterns has been computed for the case when the model is near the end-on position. It was postulated that the spacing between scatterers was an integral number of half wavelengths, so that complete reinforcement would occur in the end-on position, and that absolute nulls in the pattern would be observable from an infinite range. Because rotation now results in a movement of the scatterer across the antenna field it is no longer possible to use a generalized parameter for model size and a specific dimension must be selected. In the end-on position the fourth power range law may have significant effects and since these increase as the model size is decreased (see the following section) a small model, 15λ in span, was chosen. The computed patterns are given in Figure 8.

It is evident that a much shorter range suffices for accurate measurement than was the case for the broadside aspect. Then measurement at a range of $3D^2/\lambda$ (where D is the maximum model dimension) was hardly sufficient for a reasonable indication of the echoing diagram, while in the end-on position a very tolerable pattern is obtained at a range of $0.75D^2/\lambda$ (i.e., $p = 0.75$).

The suspicion arises that if the minimum tolerable range is to be defined as pD^2/λ, D should not be the maximum target dimension but should possibly be this dimension projected in the antenna plane. That caution is required in the acceptance of this idea is indicated in Figure 8b where points are interpolated to indicate what the pattern would have been if the radar fourth power law could have been neglected. Nulls are modified by both phase front curvature and by the effects of the radar fourth power law,* and acceptance of a criterion based on projected area may lead to the choice of a range where the latter predominates. An attempt will be made in the following section to formulate the influence of both effects on a range criterion.

The Development of a Criterion for Test Range

The preceding discussion has recognized three factors which cause distortion in the measurement of an echoing pattern. They are:

(a) the curvature of the radiation phase fronts at the model

(b) the variation in incident amplitude across the model

(c) the fact that returns from the nearer parts of the model are emphasized with respect to those from more distant parts (the fourth power law effect).

---

*At ranges greater than d^2/λ, where d is the antenna diameter, the fall off in return power P with range R is accurately represented by $P \propto R^{-4}$. At much smaller ranges $P \propto R^{-2}$ is a more realistic formulation. A plot of the on-axis gain of the uniformly illuminated antenna considered in this report is given in Figure 9.

The impression has been created that of these, the first is by far the most important. It would appear to make it necessary to demand a measurement range so great that effect (b) is negligible (see Figures 6 , 7). In this section further ideas with respect to factors (a) and (c) will be developed, with the object of setting up rules governing the necessary antenna to model range. A perusal of Figures 6 and 7 indicates that there is no problem in determining the pattern where the component signals reinforce one another; the difficulty is one of resolving minima. Therefore the simplest possible model exhibiting the distortion of minima by factors (a) and (c) will be analyzed, so that the effects of changing the model size $a\lambda$, and the range factor p may be better appreciated. It will be assumed throughout that the target is at such a range that wavefronts may be assumed spherical. Consider the three point model shown in sketch B.

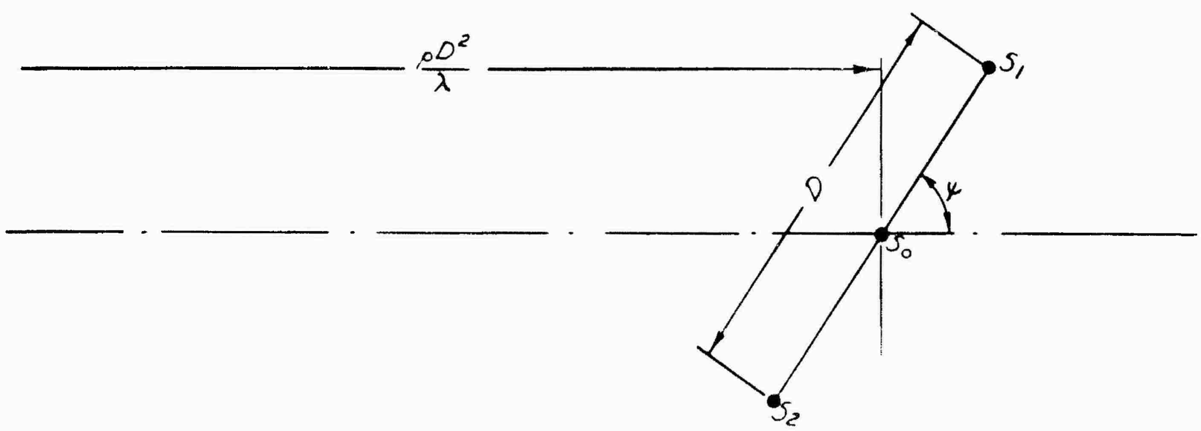

SKETCH B

This exhibits both factors, since the curvature of the incident phase front modifies the phase of returns from the outer scatterer with respect to that from the inner, while except in the broadside position a stronger return will be obtained from one outer scatterer than from the other. In Appendix B the magnitude of the signal at the free space null position is independently formulated for each factor and it is shown that, provided p is of the order of 3 or more, and that D/λ is greater than about 5:

(a) $\dfrac{\text{Magnitude of phase front curvature null}}{\text{Signal maximum}} = n_p = \dfrac{\pi}{6\rho} \sin^2 \psi$ (2)

(b) $\dfrac{\text{Magnitude of 4th power law null}}{\text{Signal maximum}} = n_f = \dfrac{\cos \psi}{\sqrt{3} \rho D/\lambda}$ (3)

Now it may be argued that the free space pattern of any target consisting of point scatterers may be regarded as a complex of arrays similar to that just considered, plus a number of other components which do not themselves result in perfect nulls. At closer range the former components would be expected to produce the greater part of the pattern distortion. Suppose that a series of echoing pattern measurements were made at a number of ranges against a line target around the broadside aspect, and examination of these patterns (e.g., Figures 6, 7) led to the conclusion that satisfactory resolution was obtained at a range of say $\rho_1 D^2/\lambda$. Then, since $\psi \doteq 90°$ the null error produced by the triplet of scatterers formulated above would be $\pi/6\rho_1$, and other triplets with smaller spacings would produce lesser errors. If then it were required to measure the pattern only within an angle of say ψ_o from the end-on position, and that the same distortion as before were acceptable, the null magnitude from the triplet considered would be unaltered if the range R were reduced to R $\sin^2 \psi_o$ (see Equation 2), provided the fourth power law term of Equation (3) is negligible, as would be the case when D/λ is very large. The contributions from other triplets would be reduced by the same factor if they were in line with the axis.

Thus, with the above qualification, a new range

$$R' = R \sin^2 \psi_o = \frac{\rho_1 D^2 \sin^2 \psi_o}{\lambda}$$

would provide a pattern of at least the same quality as that measured at a range $\rho D^2/\lambda$ against a broadside target.

Now $D \sin \psi_o$ (= say D_p) is the maximum length of the target projected in the antenna plane for the measurement considered, so that:

$$R' = \frac{\rho_1 D_p^2}{\lambda} \quad (4)$$

An obvious difficulty is that, while the formula may be quite satisfactory with a large target inclined at a considerable angle to the antenna axis, its direct application when only head-on measurements are to be made may suggest a range so small that fourth power law errors predominate. It will now be shown that the attractive simplicity of the formula may be retained and its validity extended, by a rider that if the computed range falls below a certain value, this value should be employed.

In fact the separately computed magnitude of the fourth power law contribution to the null error may be directly added to or subtracted from that due to phase front curvature effects. For it is shown in Appendix A that, provided the value of p is greater than about 3 (as an examination of Figures 5 and 6 would justify) and if D/λ is of the order of 10 or more, the magnitude modification of the close range pattern by each of these effects may be represented by vectors at 90° from the return from the center scatterer. In alternate nulls these will add, and then the total null magnitude is:

$$n = n_p + n_f = \frac{\pi}{6p}\sin^2\psi\left(1+\frac{6\lambda}{\sqrt{3\pi D}}\,\frac{\cos\psi}{\sin^4\psi}\right) \quad (6)$$

This function, together with its components, is sketched below.

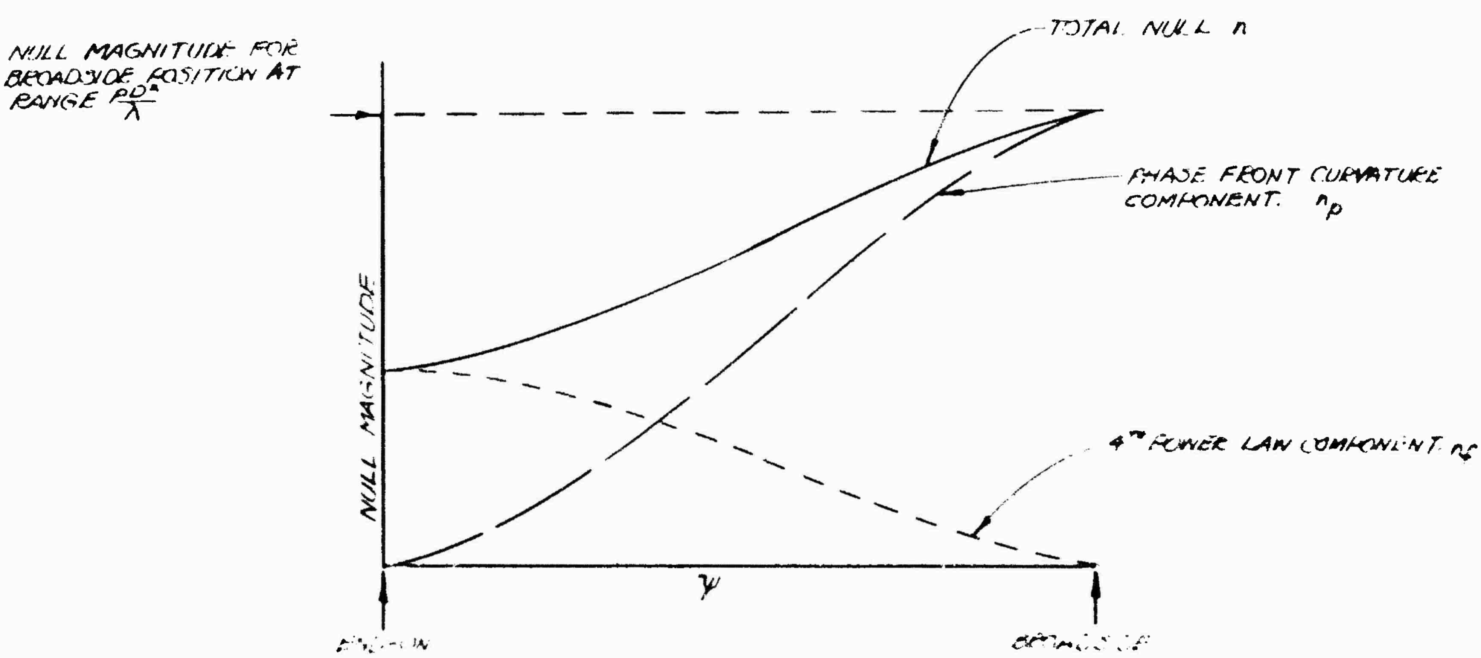

On this basis the pattern from a range $\rho D_p^2/\lambda$ will never be so good as the equivalent broadside pattern at $\rho D^2/\lambda$. But provided the additional error is small the projected length criterion, which allows a significant decrease in range as compared with $\rho D^2/\lambda$, is acceptable. Now let us ask how small an angle of target inclination from the end-on position (ψ_o) may be utilized in the criterion before the null error is increased by more than a factor of $1 + K$ where K is an arbitrarily chosen number which represents the maximum increase in null amplitude that is to be allowed as a result of fourth power law effects.

From equation (6) the fractional increase in the null resulting from the introduction of the fourth power law term is $6\lambda \cos\psi_o / \sqrt{3}\,\pi D \sin^2\psi_o$. Setting this equal to K, we obtain:

$$\sin^2\psi_o = \frac{6}{(\pi K)^2}\left(\frac{\lambda}{D}\right)^2\left[\sqrt{1+\frac{(\pi K)^2}{3}\left(\frac{D}{\lambda}\right)^2} - 1\right]$$

For example, if a K of 0.26, or a 2 db increase in null level, is acceptable:

$$\sin^2\psi_o = \frac{9.0}{(D/\lambda)^2}\left[\sqrt{1+.22\left(\frac{D}{\lambda}\right)^2} - 1\right]$$

If D/λ has a value greater than 5, the square root term may be written as $0.48D/\lambda$ with an error of less than 5%, and the value of $\sin^2\psi_o$ will then be accurate to better than 10%. Thus,

$$\sin^2\psi_o \approx \frac{9}{(D/\lambda)^2}\left[0.48\frac{D}{\lambda} - 1\right] = \frac{1}{D/\lambda}\left[4.3 - \frac{9}{D/\lambda}\right]$$

If projected area were based on a closer approach to the end-on position than ψ_o the range computed using the projected area formula would be so small that fourth power law effects would predominate. If this is not to be the case and an increase in null level of 2 db is acceptable the minimum allowed range $\rho D_p/\lambda$ becomes:

$$\frac{\rho D^2}{\lambda} \cdot \frac{1}{D/\lambda}\left(4.3 - \frac{9}{D/\lambda}\right) \approx 4.3\,\rho D\left(1 - \frac{2}{D/\lambda}\right)$$

We may assume that there is little virtue in requiring a smaller error in the null than this, so the above minimum range formula provides a basis for a working rule. Since the 2 db criterion is very arbitrary there is little harm in introducing a further simplification. Let the term $2/D/\lambda$ be ignored; this requires an increase in minimum range of only 20% for a 10λ model. Further, in order to eliminate significant figures which cannot be justified by the manner in which the allowed 2 db error was chosen, let the factor 4.3 be rounded to 5. Thus, with a number of qualifications, a tentative working rule for obtaining the range necessary for satisfactory measurement of the echoing pattern of a target is: First, on the basis of calculations (e.g., Figures 5 and 6) or experimental measurements, decide upon a factor p, which allows satisfactory resolution of the broadside pattern of a model at a range $\rho D^2/\lambda$, where D is the maximum target dimension. Then for an equally satisfactory pattern resolution at any other aspect, the test range must be $\rho D_p^2/\lambda$ where D_p is the maximum target dimension projected in the antenna plane, or $5\rho D$, whichever is the greater.

Because this rule is based on the assumption of spherical wave fronts at the target, its validity is not easy to establish generally for the case when the test range is less than d^2/λ, where d is the antenna diameter. That it is possible at times to work below this limit is illustrated in Figure 8. At present all that can be said is that the rule is certainly valid for small antennae. The point will be examined in detail in a later report. A further doubt lies in the apprehension that a long target seen end-on may present a capture cross-section greater than the beam dimension at the range allowed by the $5\rho D$ rule. The following section provides reassurance on this point.

The Range Criterion in Relation to a Target Having an Echoing Area Larger than its Presented Area

An end fire antenna has a capture cross-section much larger than its presented area, and the possibility must be faced that a long target will show an analogous property when viewed end-on, if the presumption that it consists only of independent point scatterers is not fulfilled. In effect the incident radiation may then converge on the target, as though the target region had lens-like properties. The question arises as to whether the illuminating radiation in an echoing-area test equipment is then of sufficient extent to prevent the introduction of errors resulting from radiation being gathered from the edges of the illuminating beam. An exact solution to this problem is very difficult -- both from the point of view of inventing an appropriate target model, and in the solution of the resulting electromagnetic field equations. But if it is assumed that the relatively random configuration of a real target will not exhibit radiation gathering effects to the same degree as a well designed end-fire antenna, a demonstration that the capture cross-section of the antenna is significantly less than the area of the incident beam will indicate that such effects are negligible for the target. That this is the case will now be shown.

Assume the target to be an end-fire antenna having n elements placed a quarter of a wavelength apart. Reference 4 indicates that such an antenna has a gain equal to the number of elements, so that if it has a length D, its gain is $4D/\lambda$. Thus its capture cross-section A_c is:

$$A_c = \frac{\lambda^2}{4\pi}\frac{4D}{\lambda}$$

If the illuminating antenna has a diameter c times the maximum target model dimension, i.e., cD, its free space half power beamwidth is approximately λ/cD. At close range the beam will be broader than this, but since taking the free space width will provide a conservative answer to the present problem, let the beam area A_b at a range R be formulated using this value.

Then $$A_b = \frac{\pi}{4}\left(\frac{R}{cD/\lambda}\right)^2$$

Our criterion allows a minimum range 5pD, and at this range:

$$A_b = \frac{\pi}{4}\left(\frac{5p\lambda}{c}\right)^2$$

Thus the ratio of target cross-section to beam area is:

$$\frac{A_c}{A_b} = \frac{D}{\lambda}\left(\frac{2c}{5\pi p}\right)^2$$

If $c = 1$, $D/\lambda = 100$ and $p = 3$

$$\frac{A_c}{A_b} = 0.18$$

Thus the diameter of the capture cross-section for this severe case is less than half that of the beam.

In fact c would then have to be increased to

$$\frac{5\pi p}{2\sqrt{D/\lambda}} = 2.6$$

before the capture cross-sections were equal. It must be therefore concluded that intercoupling effects within a target are unlikely to result in measurement errors at the formulated range unless an antenna larger than the maximum model dimension is employed.

Some Numerical Examples of Test Range

An examination of Figures 6 and 7 suggests that an unsatisfactory measurement is likely to result if a value of p of less than 3 is employed in the range criterion. So that the length of the test range may be appreciated some specific values associated with varying target size and aspect at a wavelength of 0.1 ft. (X-band) are tabulated below:

Target Dimension in Wavelengths D/λ	Test Range in feet ($p = 3.$ $\lambda = 0.1$ ft.)			
	Broadside Aspect	Within 45° of end-on	Within 30° of end-on	End-on Aspect
10	30	15	15	15
20	120	60	30	30
40	480	240	120	60
70	1,470	735	368	105
100	3,000	1,500	750	150
200	12,000	3,000	1,500	300
300	27,000	13,500	6,750	450

This is illustrative of both the very large range required for measurement in the broadside position, and the great improvement that is obtainable if measurements may be restricted to near the end-on aspect. It should be noted that the required range is proportional to test wavelength in all cases, so that possibility exists of obtaining satisfactory patterns against large models at one third of the range shown above if K-band radiation is used; even so, the length of the test site is uncomfortably great when the target is longer than about 50λ . It is for measurements against such large targets that the alternative approach (mentioned in the Introduction) of designing a special antenna capable of reproducing far-field conditions in its near zone is most likely to be justified.

Conclusions

By postulating a target consisting of an array of point scatterers, a criterion has been derived to define the range required between a radar and a target model whose echoing area is to be measured. The criterion is applicable provided the maximum target dimension is at least 10 wavelengths, and is:

Let D be the maximum dimension of the model, D_p be its maximum projected dimension as seen by the test antenna, λ the test wavelength, and p a number of the order of 3 which defines the measurement quality to be obtained. Then the required test range R is given by the greater of:

$$R = \frac{pD_p^2}{\lambda}$$

or: $$R = 5pD$$

The quality of measurement associated with specified values of p is indicated in Figures 6 and 7. These provide computed patterns plotted near the broadside aspect of a simplified target containing five point scatterers which exhibits perfect nulls in its infinite range echoing pattern. At a lesser range pD^2/λ such nulls become minima having in this case the levels tabulated below:

p	Minimum in db below pattern maximum
2	-13 db
3	-17 db
6	-22 db
10	-27 db

The criterion has been developed by recognizing that:

(a) At ranges greater than about $2D^2/\lambda$ there is little variation in the intensity of illumination across the model span, provided that the antenna diameter is no larger than the model span.

(b) Except near the end-on aspect the majority of the echoing pattern distortion results from variation of the phase of the incident illumination across the model. By noting that phase front contours are practically circular at ranges greater than d^2/λ (where d is the antenna diameter) a simple formulation of the range dependence of phase deviation, and hence echoing pattern distortion is possible.

(c) If the $\rho D_\rho^2/\lambda$ criterion were employed when the target was viewed end-on the range indicated might be so short that the pattern errors might be materially increased from overweighting of the returns from the near end of the target consequent upon the inverse fourth power of range law for radar returns. By limiting the minimum range to $5\rho D$ such effects are made negligible.

The qualifications implicit in the criterion are therefore:

(1) The antenna diameter should be no greater than the maximum target dimension.

(2) It is not yet clear that a range less than d^2/λ is acceptable. (d = antenna diameter.)

Examination of a case where the presumption that the target consists of separate scatterers is not met indicates that such a condition is unlikely to invalidate the rule.

When the criterion is applied to targets larger than 50 wavelengths, uncomfortably large test ranges are indicated. It is for measurements against such targets that the design of an antenna capable of reproducing far field conditions in its near zone should be studied.

References

1. Fails, W. A. & Fubini, E. G.; Methods of Measuring Radar Cross Sections; Airborne Instruments Laboratory, Inc. Report No. 380-1 (ATI 49460); January 1949.

2. Melling, W. P.; Factors Affecting the Choice of a Radar System for the Measurement of Echoing Area; to be published as a Cornell Aeronautical Laboratory report under Contract DA-30-115-ORD-739.

3. Woonton, G. A., Hay, D. R. & Logan, E. L.; An Experimental Investigation of Formulas for the Prediction of Horn Radiator Patterns; Journal of Applied Physics, Volume 20, p. 71; 1949

4. Silver, S.; Microwave Antenna Theory and Design; McGraw-Hill; p. 275.

FIG. 1 SYSTEM GEOMETRY

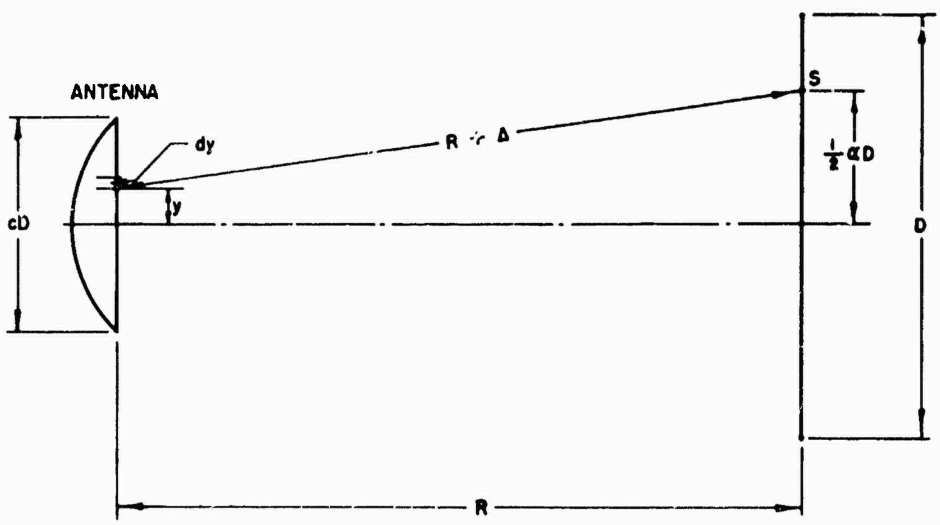

LET PATH INCREMENT Δ IN OFF-AXIS RANGE RESULT IN PHASE LAG $\frac{\phi'}{2}$

$$\frac{\phi'}{2} = \frac{2\pi}{\lambda}\left[\sqrt{R^2 + (\tfrac{1}{2}\alpha D - y)^2} - R\right]$$

$$\approx \frac{\pi}{\lambda R}\left(\tfrac{1}{2}\alpha D - y\right)^2 \qquad \text{PROVIDED } \frac{\pi R}{4\lambda}\left(\frac{\tfrac{1}{2}\alpha D - y}{R}\right)^4 \ll \text{SAY } \frac{\pi}{2}$$

$$\text{I.e. AT EXTREME } \quad \frac{1}{2}\frac{R}{\lambda}\left(\frac{D}{R}\right)^4 \ll 1$$

$$\text{OR} \quad \frac{1}{2p^3}\left(\frac{\lambda}{D}\right)^2 \ll 1$$

IF $R = \frac{pD^2}{\lambda}$

$$\frac{\phi'}{2} = \frac{\pi}{p}\left(\frac{1}{2}\alpha - \frac{y}{D}\right)^2$$

NET PHASE SHIFT $\phi/2$ AT DISTANCE $\frac{1}{2}\alpha D$ FROM AXIS GIVEN BY

$$\text{TAN}\,\frac{\phi}{2} = \frac{\int_{-\frac{cD}{2}}^{+\frac{cD}{2}} \text{SIN}\,\frac{\phi'}{2}\,dy}{\int_{-\frac{cD}{2}}^{+\frac{cD}{2}} \text{COS}\,\frac{\phi'}{2}\,dy} \qquad \left(\phi = \text{TOTAL PHASE SHIFT FOR GO-RETURN PATH}\right)$$

$$\text{RECEIVED AMPLITUDE (2 WAY)} \propto \left[\int_{-\frac{cD}{2}}^{+\frac{cD}{2}} \text{SIN}\,\frac{\phi'}{2}\,dy\right]^2 + \left[\int_{-\frac{cD}{2}}^{+\frac{cD}{2}} \text{COS}\,\frac{\phi'}{2}\,dy\right]^2$$

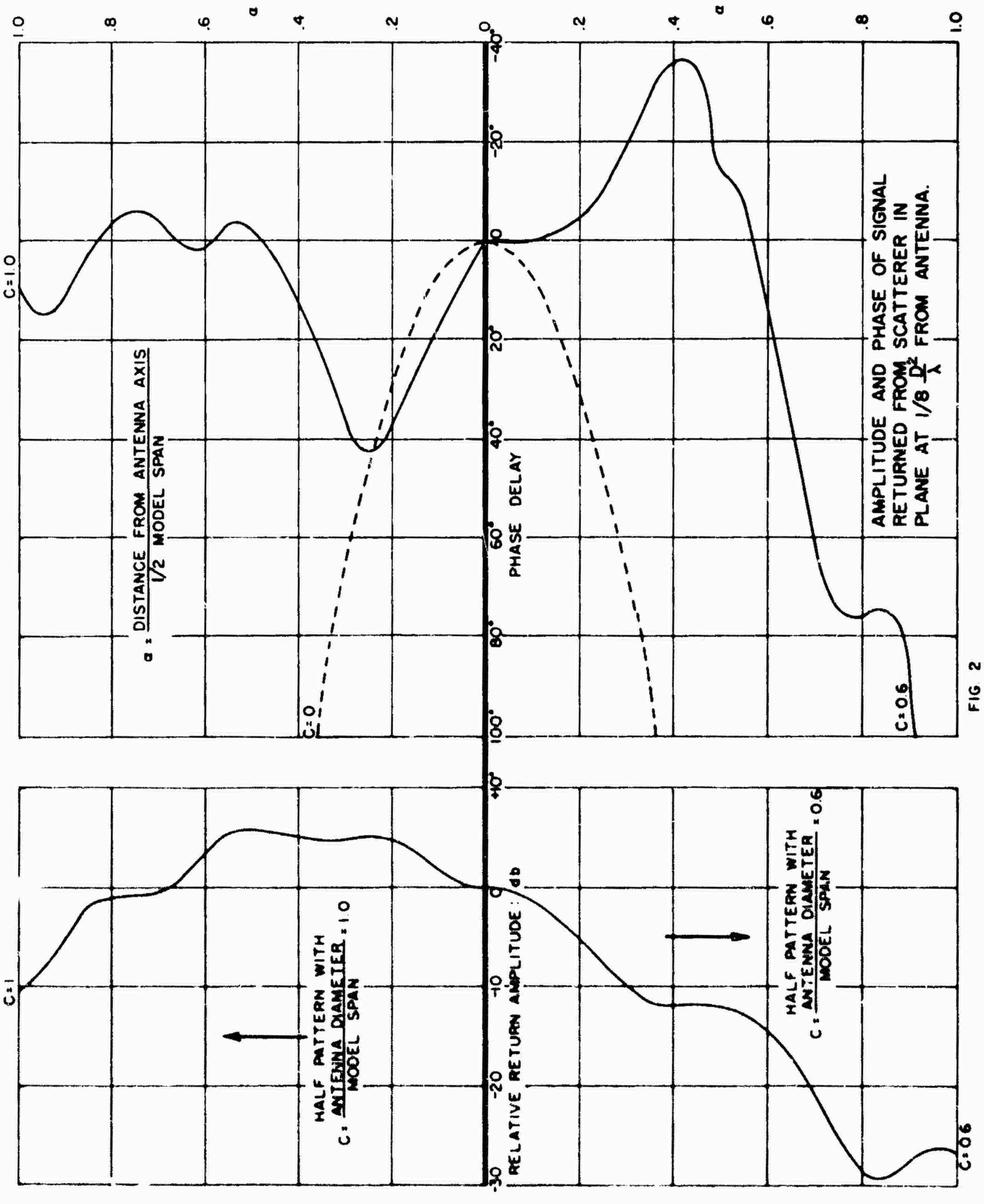

AMPLITUDE AND PHASE OF SIGNAL RETURNED FROM SCATTERER IN PLANE AT $1/8\ \frac{D^2}{\lambda}$ FROM ANTENNA.

FIG 2

UB-1088-P-100

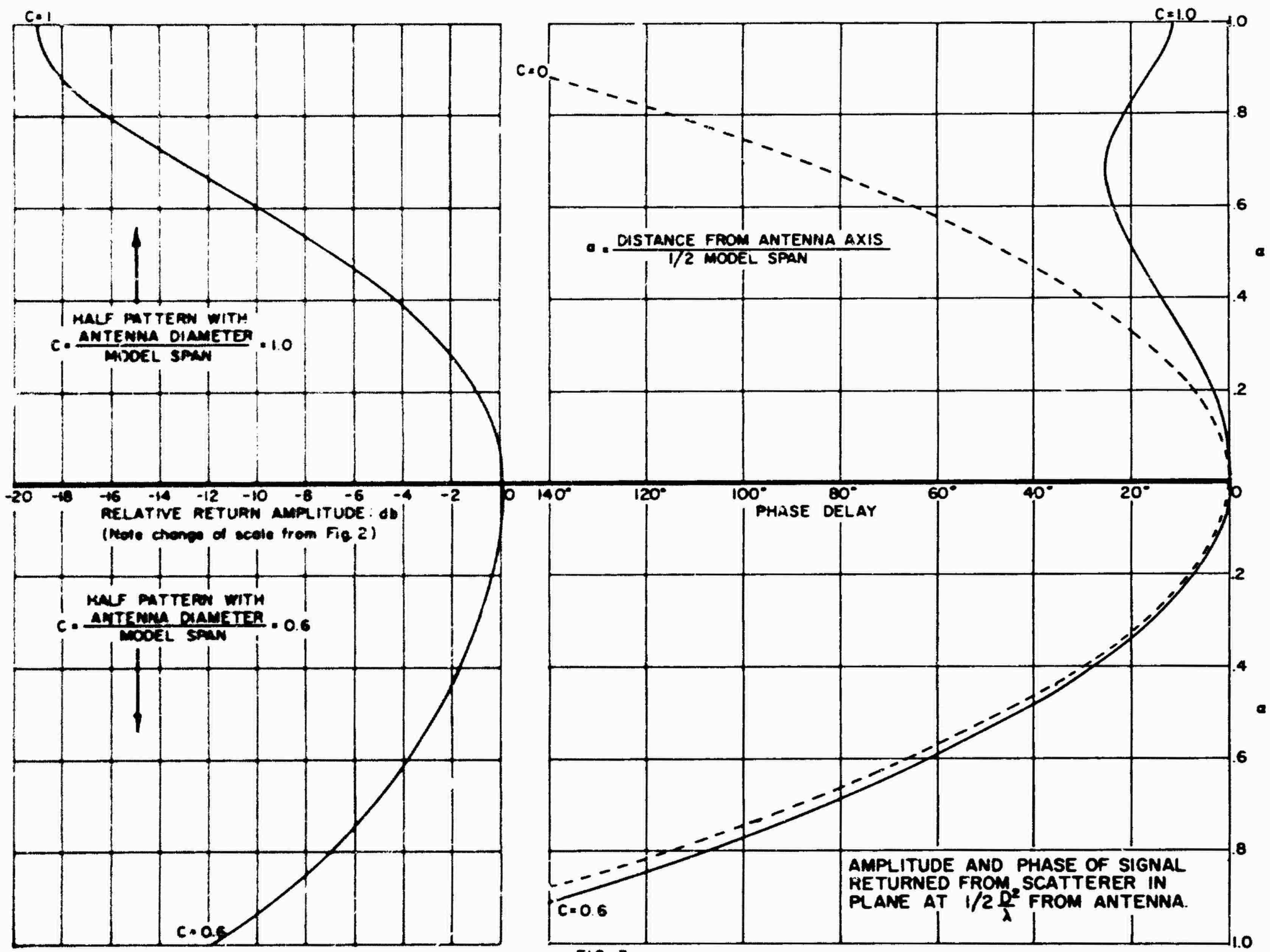
C=1
C=1.0
C=0
C=0.6
C=0.6
HALF PATTERN WITH
C = ANTENNA DIAMETER / MODEL SPAN = 1.0
HALF PATTERN WITH
C = ANTENNA DIAMETER / MODEL SPAN = 0.6
a = DISTANCE FROM ANTENNA AXIS / 1/2 MODEL SPAN
-20 -18 -16 -14 -12 -10 -8 -6 -4 -2 0
RELATIVE RETURN AMPLITUDE: db
(Note change of scale from Fig. 2)
140° 120° 100° 80° 60° 40° 20° 0
PHASE DELAY
1.0 .8 .6 .4 .2 0 .2 .4 .6 .8 1.0
a
a
AMPLITUDE AND PHASE OF SIGNAL RETURNED FROM SCATTERER IN PLANE AT $1/2 \frac{D^2}{\lambda}$ FROM ANTENNA.

FIG. 3

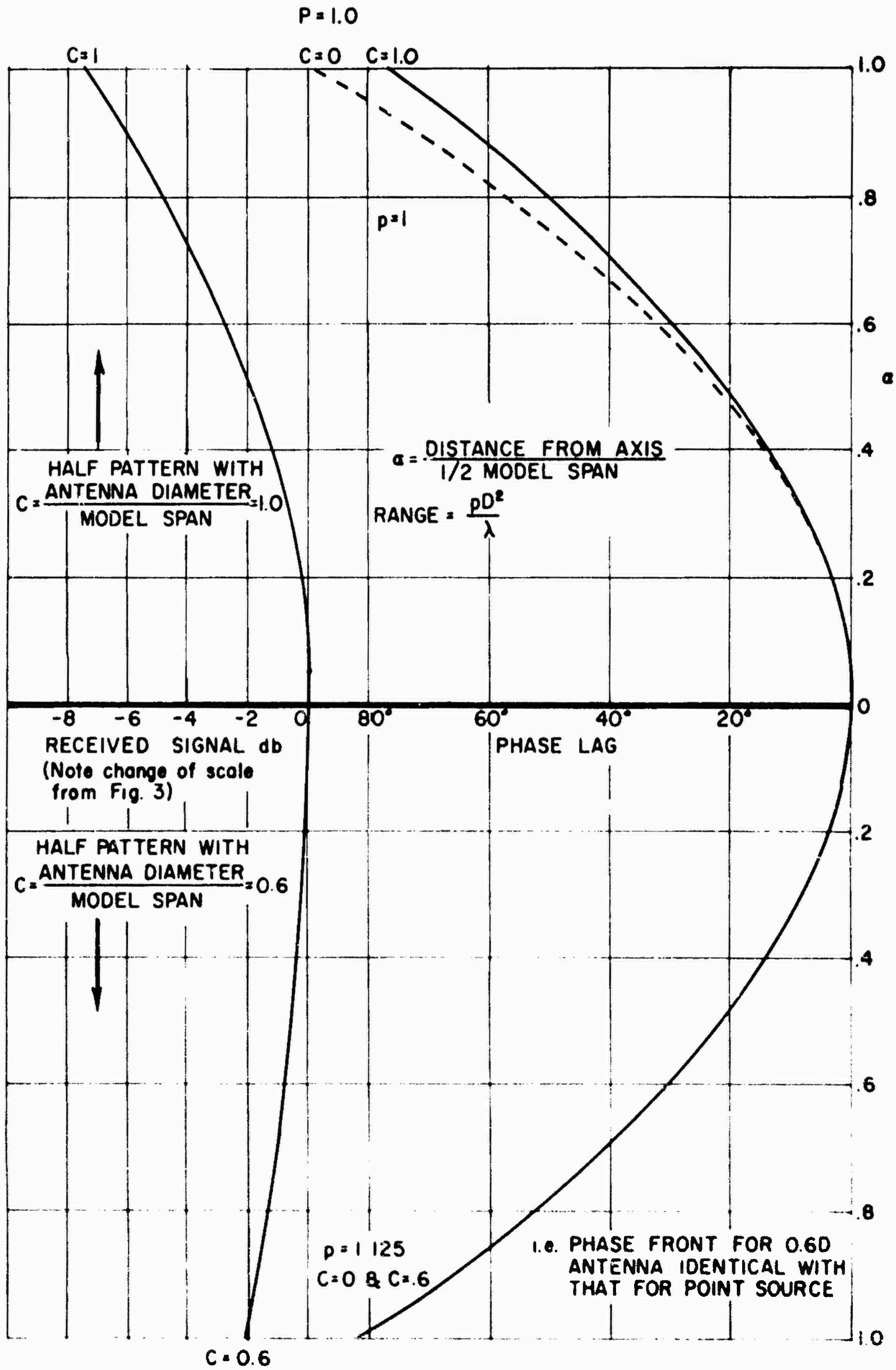

AMPLITUDE & PHASE OF SIGNAL RETURNED FROM SCATTERER IN PLANES AT 1.0 AND 1.125 D^2/λ FROM ANTENNA

FIG. 4

118-1068-P-103
276-002-23A P2

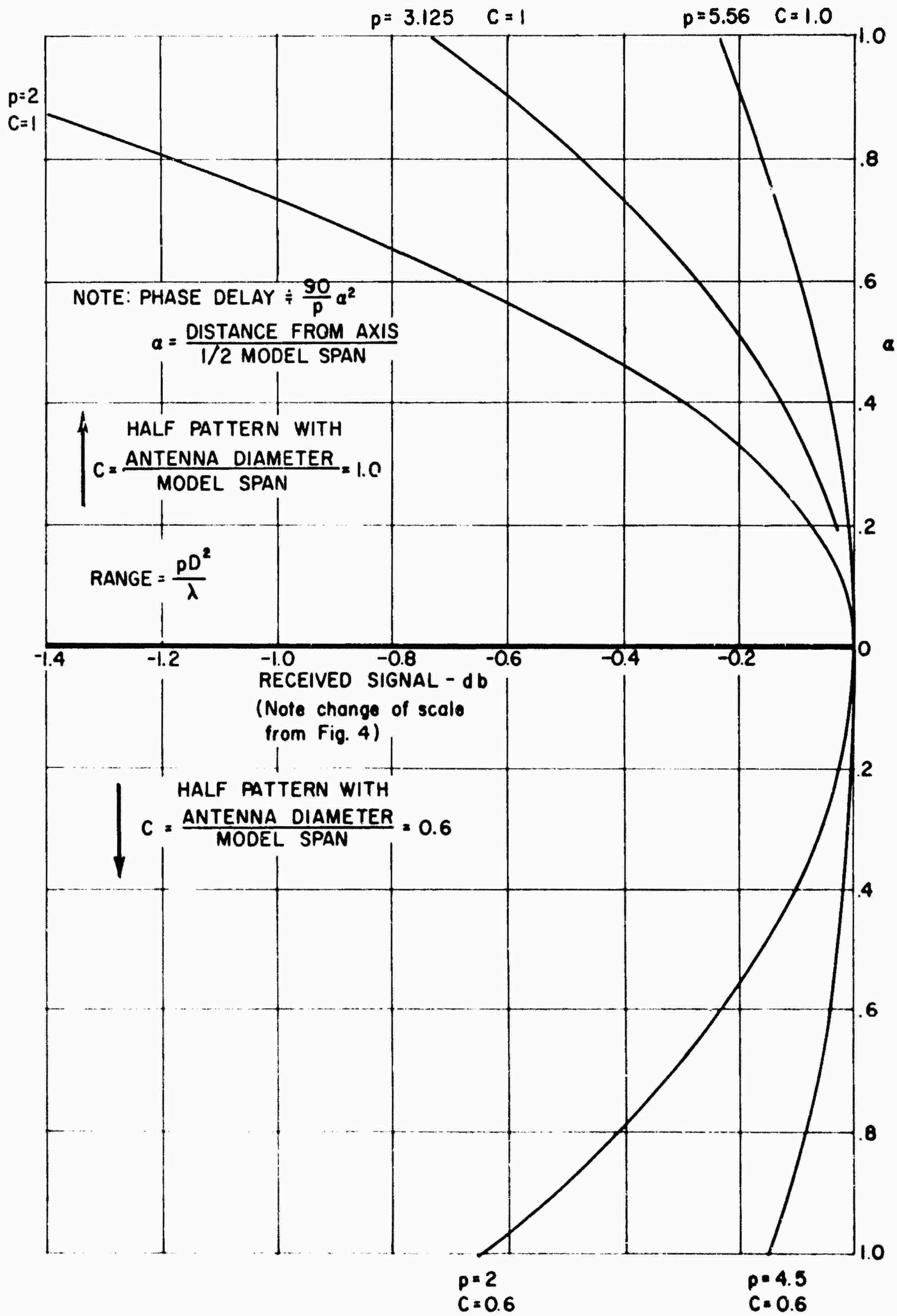

AMPLITUDE OF SIGNAL RETURNED FROM SCATTERERS IN PLANES BETWEEN 2.0 AND 5.56D^2/λ FROM ANTENNA

FIG. 5

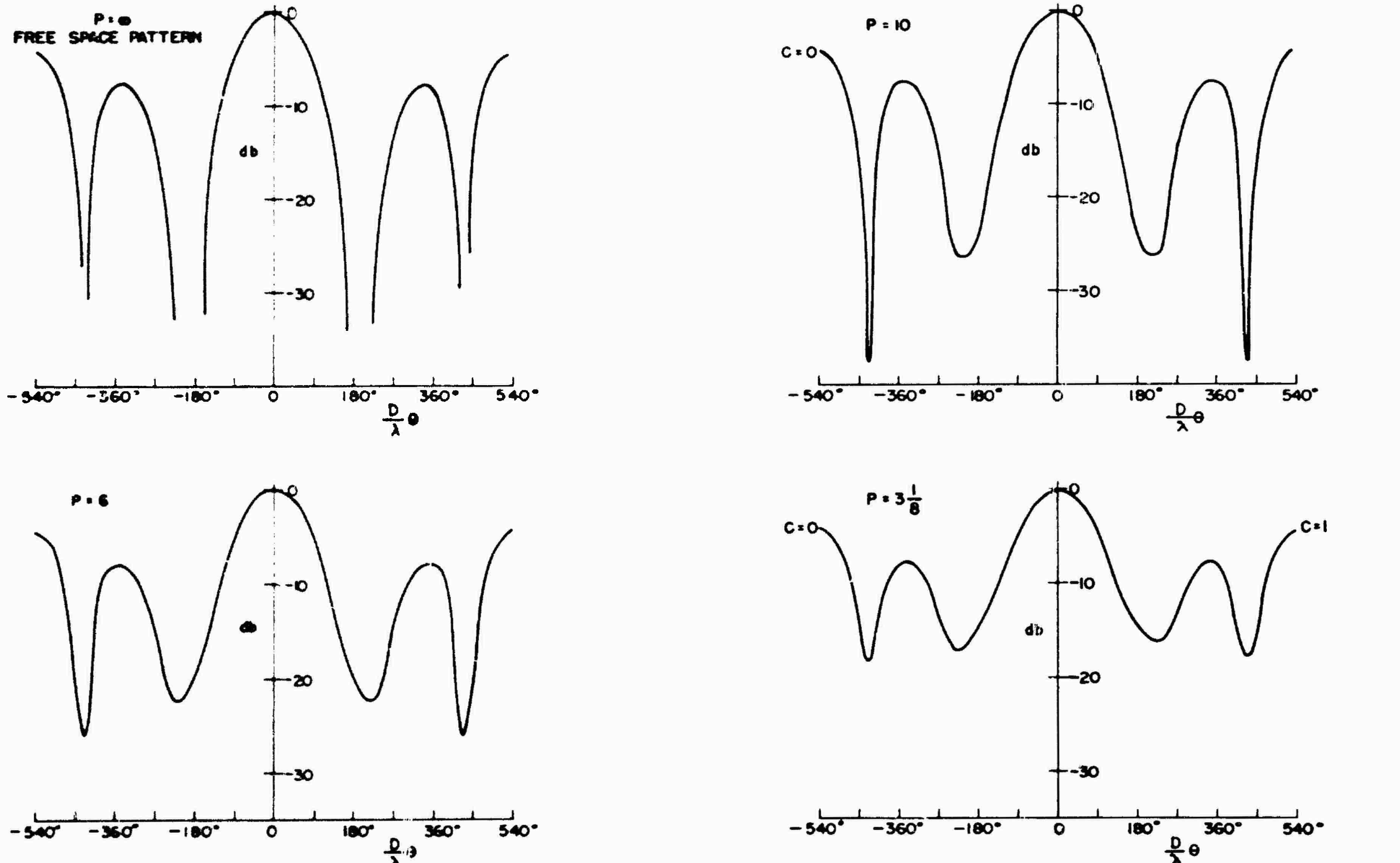

ECHOING PATTERNS OF 5-POINT MODEL NEAR BROADSIDE POSITION AT RANGE $\frac{pD^2}{\lambda}$
(p between infinity and 3)
FIG. 6

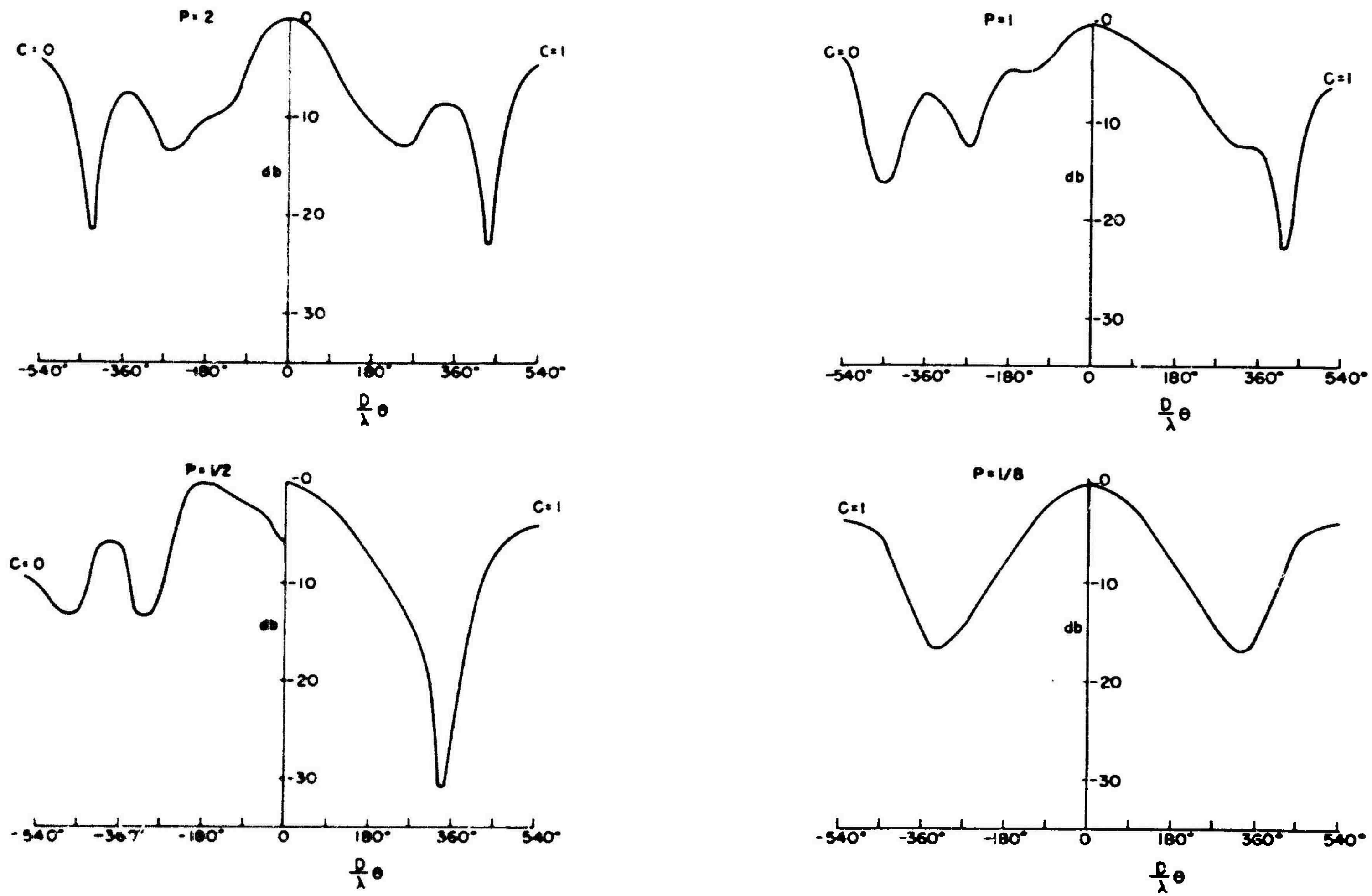

ECHOING PATTERNS OF 5 POINT MODEL (CONT'D)
FIG. 7

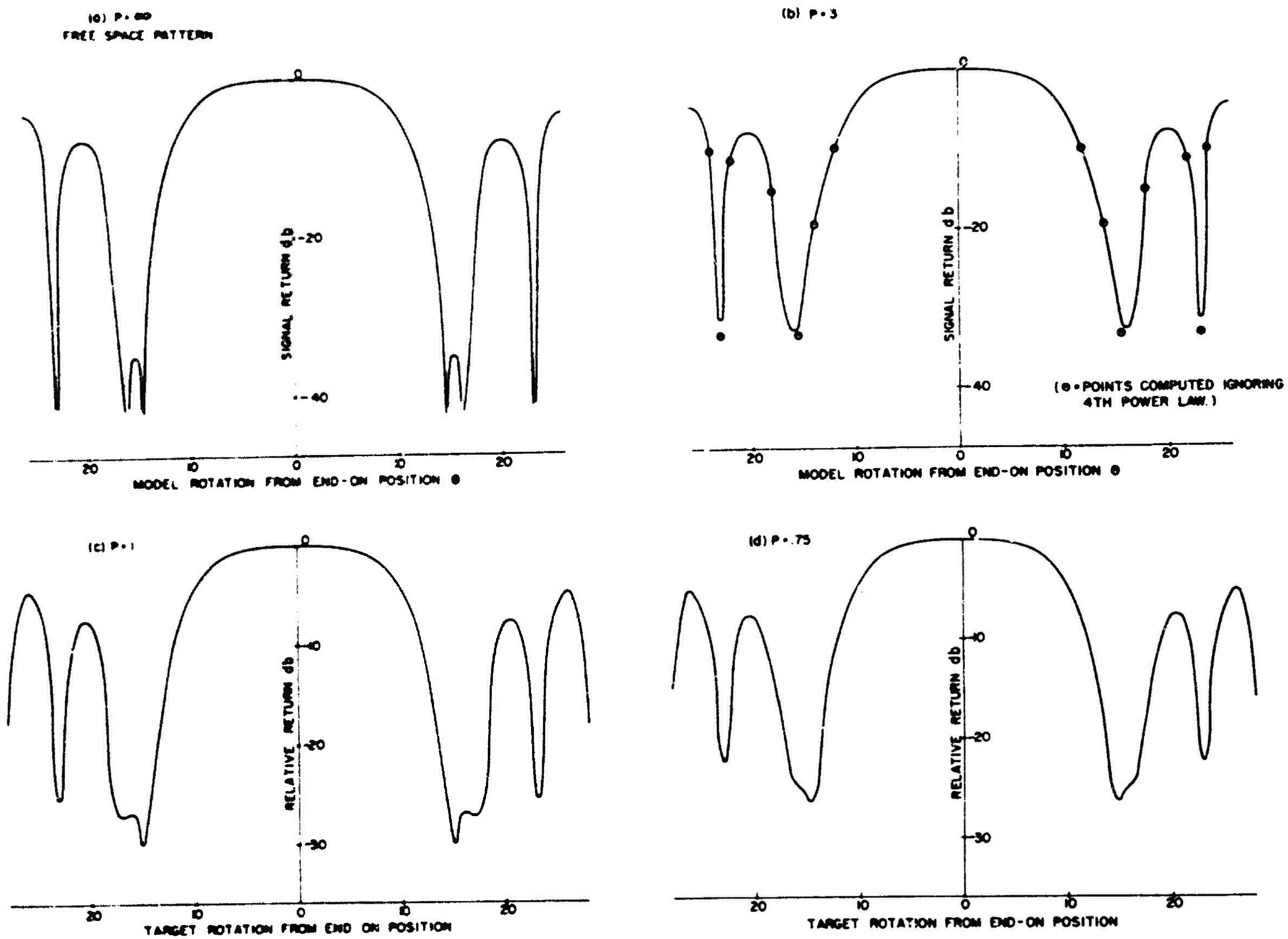

ROTATION FROM END-ON POSITION = θ
RANGE = $\frac{2D^2}{\lambda}$
MODEL LENGTH = 15λ

ECHOING PATTERNS OF FIVE POINT MODEL
NEAR END-ON POSITION

FIG. 8

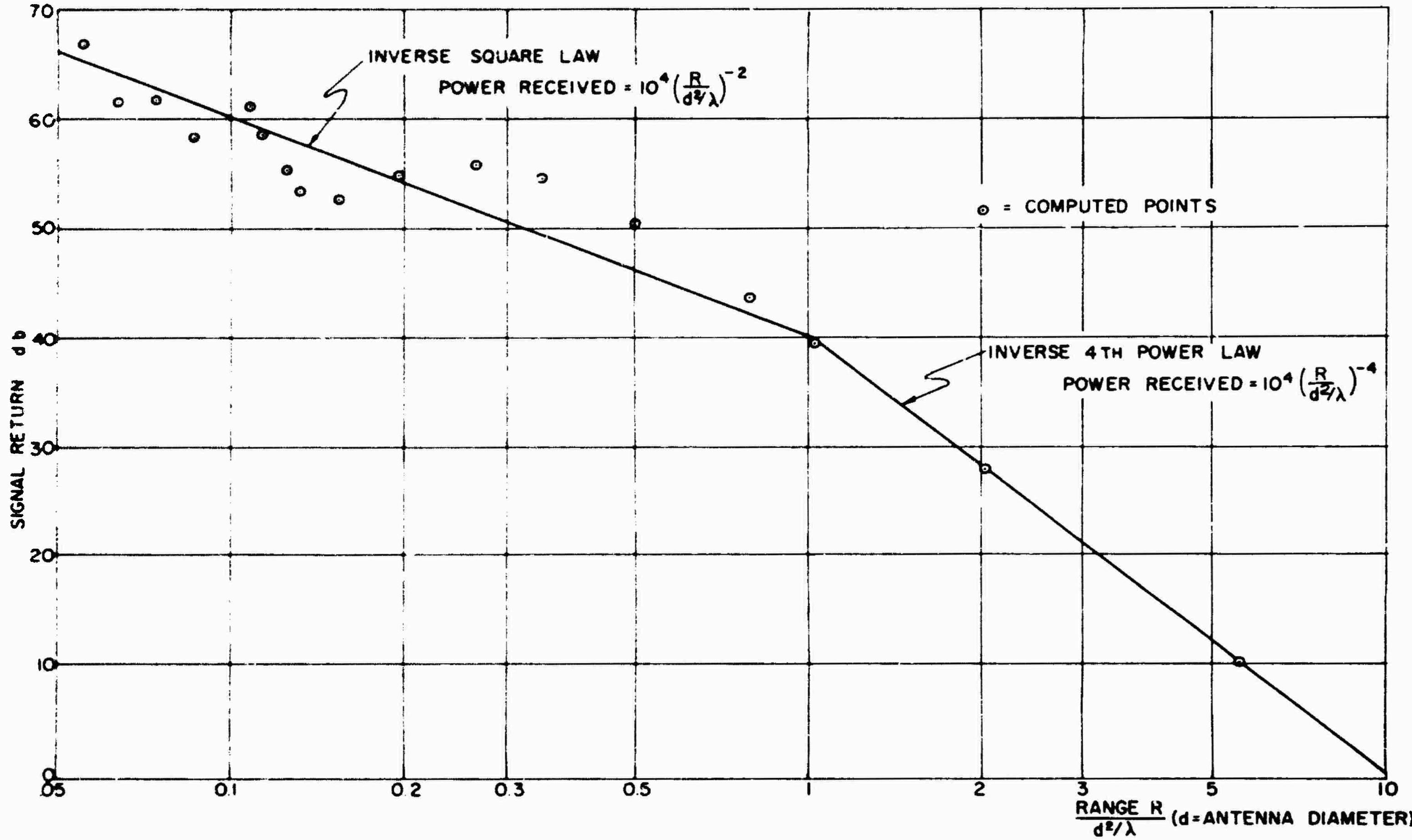

SIGNAL RETURN FROM ON-AXIS SCATTERER
AT RANGES NEAR $\frac{d^2}{\lambda}$, WHERE d = ANTENNA DIA.

FIG. 9

APPENDIX A

THE THREE SCATTERER TARGET

Let a target of span D containing only three equal symmetrically placed scatterers be considered in an analysis where the following effects are to be examined separately:

(a) Illumination phase front curvature, including the effects of the differing degrees of curvature at the near and far ends of the target

(b) Fourth power law effects.

Geometry of the Test Arrangement

Suppose the target range $\rho D_p^2/\lambda$ to be sufficient (range > d^2/λ, d being the antenna diameter) for the phase fronts to be assumed spherical. The antenna may then be regarded as a point source, and the geometry of the test configuration is that in the sketch:

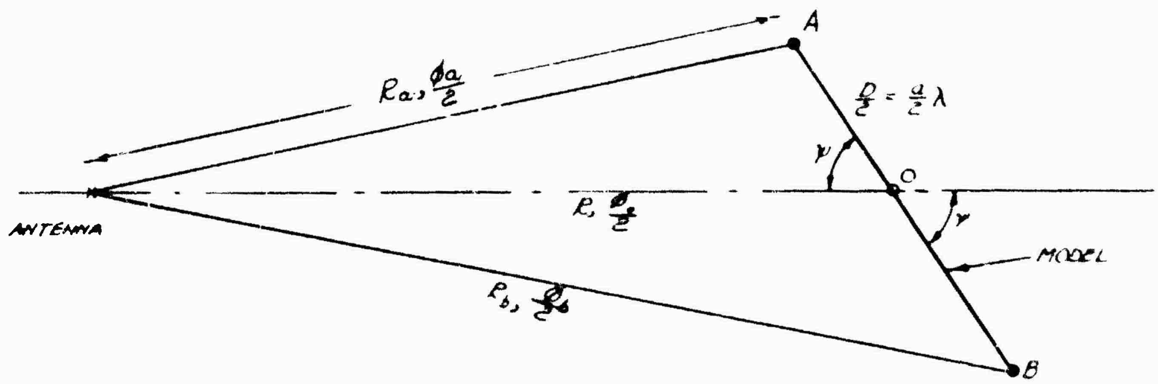

Now $$R_a = \left[(D/2)^2 + R^2 - RD\cos\psi\right]^{1/2}$$

and the phase shift ϕ_a between the transmitted signal and that received from A is $\frac{4\pi}{\lambda} R_a$

and if $R = \rho D^2/\lambda$ and $D = a\lambda$

$$\phi_a = \frac{4\pi}{\lambda}\left[\frac{(a\lambda)^2}{4} + \rho^2 a^4 \lambda^2 - \rho a^3 \lambda^2 \cos\psi\right]^{1/2}$$

$$= 4\pi\rho a^2\left[1 - \frac{\cos\psi}{\rho a} + \frac{1}{4\rho^2 a^2}\right]^{1/2}$$

Similarly

$$\phi_b = 4\pi\rho a^2\left[1 + \frac{\cos\psi}{\rho a} + \frac{1}{4\rho^2 a^2}\right]^{1/2}$$

and

$$\phi_o = 4\pi\rho a^2$$

Now let the phase of returns from A and B be referred to that of the center point 0, so that

$$\phi_A = \phi_a - \phi_o$$

$$\phi_B = \phi_b - \phi_o$$

(so that ϕ_A is positive when the phase of the return from A lags on that from 0).

Now

$$\phi_A = \frac{\phi_a^2 - \phi_o^2}{\phi_a + \phi_o} = \frac{-4\pi\rho a^2\left[\frac{\cos\psi}{\rho a} - \frac{1}{4\rho^2 a^2}\right]}{1 + (1-n)^{1/2}} \qquad (1)$$

where

$$n = \frac{\cos\psi}{\rho a} - \frac{1}{4\rho^2 a^2}$$

Similarly

$$\phi_B = \frac{+4\pi\rho a^2\left[\frac{\cos\psi}{\rho a} + \frac{1}{4\rho^2 a^2}\right]}{1+(1-y)^{\frac{1}{2}}} \tag{2}$$

where $y = -\frac{\cos\psi}{\rho a} - \frac{1}{4\rho^2 a^2}$

The Free Space Pattern

At infinite range $\frac{1}{\rho a} = 0 \quad (a = \frac{D}{\lambda})$

Then

$$\begin{aligned} \phi_{A1} &= -2\pi a \cos\psi \\ \phi_{B1} &= +2\pi a \cos\psi \\ \phi_0 &= 0 \end{aligned} \tag{3}$$

Then, assuming each scatterer to have the same reflectivity, the received signal may be represented as the sum of 3 components of equal amplitude

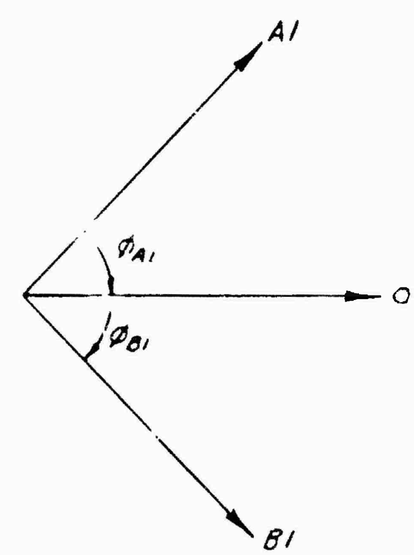

and the pattern will exhibit perfect nulls when

$$\cos \phi_{A1} = \cos \phi_{B1} = -0.5$$

and $$\sin \phi_{A1} = -\sin \phi_{B1} = \pm \sqrt{3}/2$$

i.e., when $-\phi_{A1} = \phi_{B1} = \frac{\pi}{3} + 2n\pi$ or $\frac{2\pi}{3} + 2n\pi$ (n an integer)

and $\cos \psi = \frac{1}{a}\left(n + \frac{1}{6}\right)$ and $\frac{1}{a}\left(n + \frac{1}{3}\right)$

The Pattern at Finite Range when the Fourth Power Law is Ignored

The next step is to ask how the nulls will be modified at a finite range. At this stage let effects resulting from the relative amplitude of returns from the three scatterers being modified as a result of the radar fourth power law be ignored. Then the modification results only from changes in the phase angle of returns from A and B.

If the return from scatterer 0 provides the phase reference we may write

$$\phi_A = \phi_{A1} + \delta_A$$
$$\phi_B = \phi_{B1} + \delta_B$$

In Equations (1) and (2) n and y are small quantities if pa is large, and a series expansion yields, in combination with Equation (3):

$$\delta_A = \frac{\pi}{2p} \sin^2\psi \left(1 + \frac{1}{2pa} \cos\psi + \cdots\right) \tag{4}$$

$$\delta_B = \frac{\pi}{2p} \sin^2\psi \left(1 - \frac{1}{2pa} \cos\psi + \cdots\right) \tag{5}$$

This is representative of the circular phase front postulated by employing an effective point antenna. The second terms in the respective series are indicative of the difference in phase front curvature between that at the nearer element A and that at the farther element B.

The vector diagram for the returns is modified now to

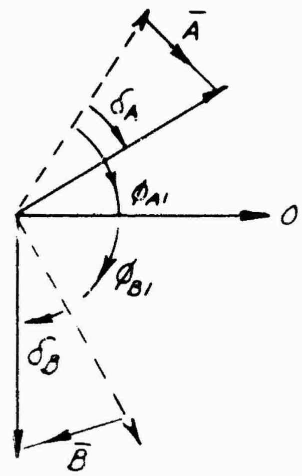

and we can express the modification to the original free-space pattern as the addition of two vectors $\bar{A}$ and $\bar{B}$. Then:

$$\bar{A} = 2\sin\frac{\delta_A}{2}\cdot e^{j\left(\phi_{A1}+\frac{\pi}{2}+\frac{\delta_A}{2}\right)}$$

$$\bar{B} = 2\sin\frac{\delta_B}{2}\cdot e^{j\left(\phi_{B1}+\frac{\pi}{2}+\frac{\delta_B}{2}\right)}$$

It has been demonstrated in the main body of the report that in the broadside aspect, where $\psi \approx 90^\circ$, p must be of the order of 3 if a reasonable measurement is to be obtained, and it is then possible to write the magnitudes $|\bar{A}|$ & $|\bar{B}|$ of the vectors as approximately δ_A and δ_B respectively.

The total disturbance Δ to the free space pattern is then:

$$\Delta = -\delta_A\sin\left(\phi_{A1}+\frac{\delta_A}{2}\right)-\delta_B\sin\left(\phi_{B1}+\frac{\delta_B}{2}\right)+j\left[\delta_A\cos\left(\phi_{A1}+\frac{\delta_A}{2}\right)+\delta_B\cos\left(\phi_{B1}+\frac{\delta_B}{2}\right)\right]$$

and since δ_A & δ_B are then small (less than about 0.5)

$$\Delta \doteq -\delta_A\left(\sin\phi_{A1}+\frac{\delta_A}{2}\cos\phi_{A1}\right)-\delta_B\left(\sin\phi_{B1}+\frac{\delta_B}{2}\cos\phi_{B1}\right)$$

$$+j\left[\delta_a\left(\cos\phi_{A1}-\frac{\delta_A}{2}\sin\phi_{A1}\right)+\delta_B\left(\cos\phi_{B1}-\frac{\delta_B}{2}\sin\phi_{B1}\right)\right]$$

and if values from Equations (3), (4) and (5) are inserted

$$\Delta \doteq \frac{\pi}{\rho} \sin^2 \psi \left\{ \left[\frac{1}{2\rho a} \sin \phi_{A1} \cos \psi - \frac{\pi}{4\rho} \sin^2 \phi_{A1} \left(1 - \frac{1}{4\rho^2 a^2} \right) \right] + j \left(\cos \phi_{A1} - \frac{\pi}{4\rho^2 a} \sin \phi_{A1} \right) \right\}$$

Now under free space conditions, pattern minimum were shown to occur when

$$\cos \phi_{A1} = -0.5 \quad \text{and} \quad \sin \phi_{A1} = \pm \frac{\sqrt{3}}{2}$$

The return at the same values of ϕ is now:

$$\frac{\pi}{\rho} \sin^2 \psi \left\{ \left[\pm \frac{\sqrt{3}}{4\rho a} - \frac{3\pi}{16\rho} \left(1 - \frac{1}{4\rho^2 a^2} \right) \right] + j \left[0.5 \mp \frac{\sqrt{3}}{8\rho^2 a} \right] \right\}$$

If a is greater than say 5, and p greater than 3 as is required for a reasonable pattern measurement, this is approximately

$$\frac{\pi}{\rho} \left(- \frac{3\pi}{16\rho} + \frac{1}{2} j \right) \sin^2 \psi$$

The real term is then a result only of the difference in phase error between the returns from scatterer A & B (i.e., it occurs because phase front curvature changes with range) while the imaginary term is caused only by the absolute phase front curvature. Referring to the free space vector diagram (page 30) it may be seen that the real term would now be cancelled at a slightly smaller value of ϕ_A (and hence a larger value of ψ) than is necessary to produce a null in free space conditions. The magnitude of the return would then be that of the imaginary component $\frac{\pi}{2\rho} \sin^2 \psi$.

At aspects where the returns reinforce the maximum magnitude of the return will be approximately 3, and we may write:

$$\frac{\text{Magnitude of phase front curvature minimum}}{\text{Magnitude of Maximum}} \doteq \frac{\pi}{6\rho} \sin^2 \psi$$

and the power ratio will be the square of this quantity.

Fourth Power Law Effects

Relative to the return from the center scatterer, the magnitude of that from A is:

$$\left(\frac{R+\frac{a\lambda}{2}\cos\psi}{R}\right)^2 \approx 1+\frac{a\lambda}{R}\cos\psi = 1+\frac{1}{pa}\cos\psi$$

while that from B is approximately

$$1-\frac{1}{pa}\cos\psi$$

If phase front curvature terms are ignored, the free space vector diagram is then modified to:

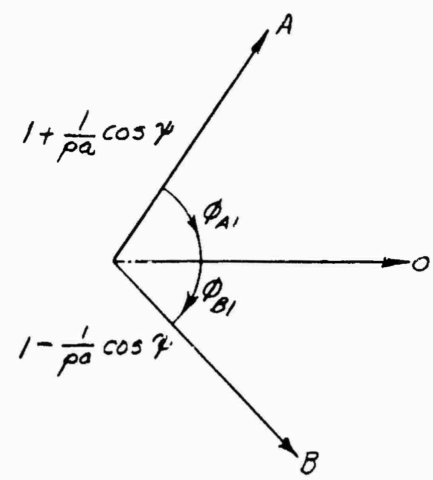

It is evident that if pa is large there will be little change in the real component of the total return as a result of the change in magnitude of its parts but that an imaginary component will result. At the nulls, where $\sin\phi_{A1} = \pm\sqrt{3}/2$, this has a magnitude $\pm\sqrt{3}\cos\psi/pa$ and comparing this with the value of 3 obtained when the total return results from signal reinforcement, we obtain:

$$\frac{\text{Magnitude of 4th power law minimum}}{\text{Magnitude of maximum}} = \frac{\cos\psi}{\sqrt{3}\,pa} = \frac{\cos\psi}{\sqrt{3}\,pD/\lambda}$$

The manner in which this modifies the disturbance to the null resulting from phase front curvature is straightforward. In the latter an imaginary component having a constant sign predominates. The fourth power law term is again imaginary, but its sign changes between successive nulls. Hence in a pattern having a fine structure the signal in successive nulls will be alternately the sum and the difference of the two terms.